

New Indicators for AGN Power: The Correlation Between [O IV] $\lambda 25.89\mu\text{m}$ and Hard X-ray Luminosity for Nearby Seyfert Galaxies

M. Meléndez, S.B. Kraemer and B.K Armentrout

Institute for Astrophysics and Computational Sciences, Department of Physics, The Catholic University of America, Washington, DC

07melendez@cua.edu

R.P. Deo and D.M. Crenshaw

Department of Physics and Astronomy, Georgia State University, Atlanta, GA

H.R. Schmitt

Remote Sensing Division, Naval Research Laboratory, Washington, DC

and

Interferometrics, Inc., Herndon, VA

R.F. Mushotzky, J. Tueller and C.B. Markwardt

NASA/Goddard Space Flight Center, Greenbelt, MD

and

L. Winter

University of Maryland, College Park, MD

ABSTRACT

We have studied the relationship between the [O IV] $\lambda 25.89\mu\text{m}$ emission line luminosities, obtained from *Spitzer* spectra, the X-ray continua in the 2-10 keV band, primarily from *ASCA*, and the 14-195 keV band obtained with the *SWIFT*/Burst Alert Telescope (BAT), for a sample of nearby ($z < 0.08$) Seyfert galaxies. For comparison, we have examined the relationship between the [O III] $\lambda 5007$, the 2-10 keV and the 14-195 keV luminosities for the same set of objects. We find that both the [O IV] and [O III] luminosities are well-correlated with the BAT luminosities. On the other hand, the [O III] luminosities are better-correlated with 2-10 keV luminosities than are those of [O IV]. When comparing

[O IV] and [O III] luminosities for the different types of galaxies, we find that the Seyfert 2’s have significantly lower [O III] to [O IV] ratios than the Seyfert 1’s. We suggest that this is due to more reddening of the narrow line region (NLR) of the Seyfert 2’s. Assuming Galactic dust to gas ratios, the average amount of extra reddening corresponds to a hydrogen column density of \sim few times 10^{21}cm^{-2} , which is a small fraction of the X-ray absorbing columns in the Seyfert 2’s. The combined effects of reddening and the X-ray absorption are the probable reason why the [O III] versus 2-10 keV correlation is better than the [O IV] versus 2-10 keV, since the [O IV] $\lambda 25.89\mu\text{m}$ emission line is much less affected by extinction. We present a grid of photoionization models used to calculate the physical conditions present in the [O IV] region. We find that the [O IV] comes from higher ionization states and lower density regions than previous studies had determined for [O III]. Overall, we find the [O IV] to be an accurate and truly isotropic indicator of the power of the AGN. This suggests that it can be useful in deconvolving the contribution of the AGN and starburst to the spectrum of Compton-thick and/or X-ray weak sources.

Subject headings: galaxies: Seyfert — X-ray:galaxies — infrared: galaxies

1. Introduction

The presence or absence of broad optical emission lines has been historically used to separate Seyfert galaxies into two classes: Seyfert 1 galaxies with broad permitted and narrow forbidden lines and Seyfert 2 galaxies with only narrow permitted and forbidden line emission (Khachikian & Weedman 1974). Using spectropolarimetry, Antonucci & Miller (1985) found broad permitted line emission in the Seyfert 2 NGC 1068 galaxy, characteristic of a Seyfert 1 spectrum. These observational results provided the first evidence in favor of a unified model. In this model (Antonucci 1993) both types of Seyfert galaxies are intrinsically the same with the differences being the visibility of the central engine. A geometrically and optically-thick dusty molecular torus-like structure surrounds the central source, as well as the broad line region (BLR). Therefore the visibility of the nuclear engine depends on the viewing angles.

Following the unified model, our line of sight to Seyfert 2 galaxies is obstructed by optically thick material corresponding to column densities of $N_H > 10^{22}\text{cm}^{-2}$ (Risaliti et al. 1999). For column densities $N_H \leq 10^{24}\text{cm}^{-2}$, photons above few keV can penetrate the torus creating an unobstructed view of the nuclear source. One refers to such cases as “Compton thin”. For values of a few times 10^{24}cm^{-2} , only high energy X-ray emission (tens of keV) can pass through the obscuring material (Turner et al. 1997). For $N_H > 10^{25}\text{cm}^{-2}$, even

high energy X-rays, above a few tens of keV, are Compton scattered and the nuclear source is completely hidden from our direct view. Therefore, in order to calculate the intrinsic luminosity for an absorbed object with $N_H > 10^{22} \text{ cm}^{-2}$, we need to find an indirect method (Mulchaey et al. 1994). Many authors have used purportedly isotropic indicators, such as the [O III] $\lambda 5007$ line (hereafter [O III]), the infrared continuum, and the 2-10 keV hard X-ray band (Heckman et al. 2005; Netzer et al. 2006; Xu et al. 1999; Alonso-Herrero et al. 1997; Horst et al. 2006). Bassani et al. (1999) presented a three-dimensional diagram for Seyfert 2 galaxies suitable to identify Compton-thick sources, using K_α iron emission line equivalent width and the 2-10 keV hard X-ray flux normalized to the [O III] line flux, with the latter corrected for extinction and assumed to be a true indicator of the intrinsic luminosity of the source.

In this paper, we present and discuss the use of [O IV] $\lambda 25.89\mu\text{m}$ (hereafter [O IV]) as an isotropic quantity avoiding the limitations of previous methods. Since it has a relatively high ionization potential (54.9 eV), it is less affected by star formation and is significantly less affected by extinction than [O III] ($A_v \sim 5 - 45$ corresponds to $A_{25.89\mu\text{m}} \sim 0.1 - 0.9$) (Genzel et al. 1998). Also, [O IV] represents an improvement over the use of infrared continuum given the difficulty in isolating the AGN continuum from the host galaxy emission (Lutz et al. 2004). For the X-ray, we choose the *Swift* Burst Alert Telescope (BAT) high Galactic latitude ($|b| > 19^\circ$) survey in the 14-195 keV band (Markwardt et al. 2005). The survey covers the whole sky at $(1 - 3) \times 10^{-11} \text{ ergs cm}^{-2} \text{ s}^{-1}$ and represents a complete sample including Compton thin AGNs that were missed from previous X-ray surveys in the 2-10 keV band because of their high column densities ($N_H \sim 10^{24} \text{ cm}^{-2}$). Furthermore, Compton-thick (i.e., $N_H \sim \text{few } 10^{24} \text{ cm}^{-2}$) sources, which cannot be detected in the 2-10 keV band by the *Advanced Satellite for Cosmology and Astrophysics* (*ASCA*), *Chandra* or *XMM-Newton*, have been detected by *Swift*/BAT (Markwardt et al. 2005; Tueller et al. 2007).

In the present work we compare the $L_{[\text{O IV}]} L_{14-195\text{keV}}$ to $L_{[\text{O III}]} L_{14-195\text{keV}}$ and $L_{[\text{O IV}]} L_{2-10\text{keV}}$ to $L_{[\text{O III}]} L_{2-10\text{keV}}$ relations for a sample of X-ray selected nearby Seyfert Galaxies. We then use the obtained relations in combination with photoionization modeling to place constraints on the physical properties in these emitting regions. We also discuss the different mechanisms behind these correlations and the possibilities of using such correlations as a way to find the intrinsic luminosity of AGNs.

2. Sample and data analysis

Using the preliminary results from the first 3 months of the *Swift*/BAT high Galactic latitude survey in the 14-195 keV band (Markwardt et al. 2005) and the new results from

the 9 month survey (Tueller et al. 2007) we have compiled a sample of 40 nearby Seyfert galaxies ($z < 0.08$, except 3C273 with $z=0.16$) for which the 2-10 keV, [O IV] $\lambda 25.89\mu\text{m}$ and [O III] $\lambda 5007$ fluxes have been measured.

The 2-10 keV fluxes are mainly from *ASCA* observations and were retrieved from the TARTARUS data base (Turner et al. 2001), except where noted in Tables 1 and 2. All the fluxes have been corrected for Galactic absorption and in the case of multiple observations, the mean flux was taken. The luminosities in the [O III] line were compiled from the literature and are presented here without reddening corrections, in Tables 1 and 2. We present [O IV] fluxes found in the literature and from our analysis of unpublished archival spectra observed with the Infrared Spectrograph (IRS) (see Houck et al. 2004) on board the *Spitzer Space Telescope* in the 1st Long-Low (LL1, $\lambda = 19.5 - 38.0 \mu\text{m}$, $10.7'' \times 168''$) IRS order in Staring mode. The [O IV] luminosities are presented without reddening corrections.

For the analysis of the archival *Spitzer* data we used the basic calibrated data (BCD) files preprocessed using the S15.3 IRS pipeline. This includes ramp fitting, dark sky subtraction, drop correction, linearity correction and wavelength and flux calibrations. The one-dimensional (1D) spectra were extracted from the IRS data using the SMART v6.2.4 data processing and analysis package (Higdon et al. 2004). For the extraction we used the “Automatic Tapered Column Point Source extraction method” for LL observations of point sources. For the LL staring mode data we performed sky subtraction by subtracting the BCDs between the two nodes after we created median BCDs from each node position. After that, the spectra from each node position for LL1 were averaged to obtain the final spectrum for that order. We performed the line fit with SMART using a polynomial to fit the continuum and a Gaussian for the line profile. NGC 6300 is the only source, within our sample, observed in high resolution with the Infrared Spectrograph (IRS) in the Long-High order (LH, $\lambda = 18.7 - 37.2 \mu\text{m}$, $11.1'' \times 22.3''$) in Staring mode. For the extraction we used the “Full” extraction method for LH observations of point sources. We created median BCDs from each node. Then the spectra from each node position for LH were averaged to obtain the final spectrum. Since background observations are not available for this galaxy and we required only the [O IV] line flux, we did not perform any background subtraction for this object.

We note the difficulty in deconvolving the adjacent [Fe II] $\lambda 25.99\mu\text{m}$ line from the [O IV] in low-resolution IRS spectra. We assumed that the fluxes measured in low-resolution mode are mostly from [O IV] given the fact that the [Fe II] is due primarily to star formation (Hartigan et al. 2004; Weedman et al. 2005; O’Halloran et al. 2006), and we have a hard X-ray BAT selected sample which is pre-selected to be sources in which the X-ray emission is dominated by an AGN. In the next section we will discuss the possible contribution of [Fe II]

to the [O IV] fluxes, based on two cases within our sample: the edge-on Seyfert 2 galaxy NGC 3079 with a nuclear starburst having a low AGN contribution (Gorjian et al. 2007) and another Seyfert 2, Mrk 3, with little or no starburst contribution (Deo et al. 2007).

All the flux errors are within 10% as obtained from the reduction package *SMART* and from the literature.

3. Results

3.1. Reddening in the NLR

In Figure 1 we compare the [O III] and the [O IV] luminosities. For our purposes, we group Seyfert 1.2’s and 1.5’s with Seyfert 1’s. From the plot we notice that Seyfert 2, Seyfert 1.9 and Seyfert 1.8 galaxies show lower [O III] luminosities than Seyfert 1 galaxies. The mean value of the luminosities our sample are: for Seyfert 1’s $\log(L_{[\text{O III}]}) = 41.4 \pm 0.9$ and $\log(L_{[\text{O IV}]}) = 41.2 \pm 0.8$, for Seyfert 1.9’s $\log(L_{[\text{O III}]}) = 40.5 \pm 0.8$ and $\log(L_{[\text{O IV}]}) = 40.9 \pm 0.4$; and for Seyfert 2’s $\log(L_{[\text{O III}]}) = 40.0 \pm 1.0$ and $\log(L_{[\text{O IV}]}) = 41.0 \pm 0.6$. A linear regression for each individual group yields a relation of the type: for Seyfert 1’s $L_{[\text{O III}]} \propto L_{[\text{O IV}]}^{0.9 \pm 0.1}$; Seyfert 1.9’s $L_{[\text{O III}]} \propto L_{[\text{O IV}]}^{2 \pm 1}$ and for Seyfert 2’s $L_{[\text{O III}]} \propto L_{[\text{O IV}]}^{1.8 \pm 0.5}$. These results are consistent with previous reports of additional reddening in the narrow line region (NLR) of Seyfert 2’s (e.g., Jackson & Browne 1991; Mulchaey et al. 1994; Keel et al. 1994; Rhee & Larkin 2005; Netzer et al. 2006).

Using the extinction law derived by Cardelli et al. (1989), the estimated extinction in the visible is $A_v \sim 1 - 6$ mag, calculated from the mean values for the [O III] luminosity required to “correct” the Seyfert 2’s (Sy1.8/1.9/2’s) [O III] to those from Seyfert 1’s, assuming a ratio of total to selective extinction of $R_v = 3.1$ (which represents a typical value for the diffuse interstellar medium). In Figure 1 we present these findings by comparing the linear regression obtained for Seyfert 1 galaxies (solid line), with those obtained for all the sample with the [O III] luminosities corrected for extinction in Seyfert 2 galaxies. Therefore, we interpreted the higher $\log(L_{[\text{O IV}]} / L_{[\text{O III}]}) \gtrsim 1$ found in Seyfert 2 galaxies to be a result of reddening.

There is a relative absence of Seyfert 1’s in nearly edge-on host galaxies (see Keel 1980; Maiolino & Rieke 1995; Schmitt et al. 2001). Our sample is consistent with this trend, in that we find that Seyfert 2’s have, on average, more inclined host galaxies with a ratio of

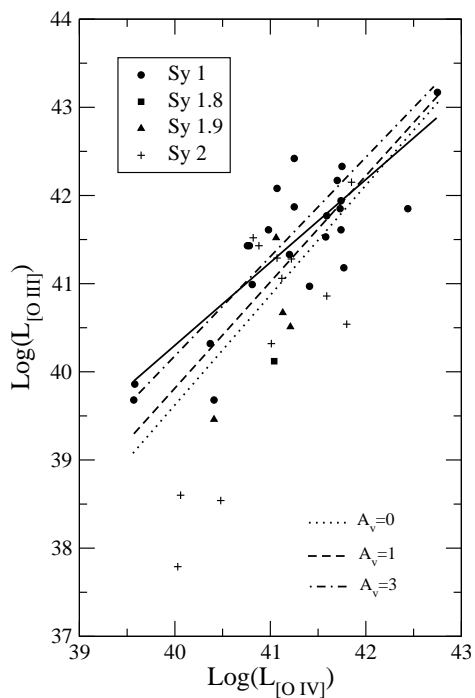


Fig. 1.— Comparison between [O IV] and [O III] luminosities. The solid line represents the linear regression calculated for Seyfert 1 galaxies; the dotted, dashed and point-dashed lines represents the linear regression for the sample with the Seyfert 2 galaxies corrected by extinction in the visible with $A_v = 0, 1$ and 3 , respectively. For comparison purposes we group Seyfert 1.8's and 1.9's with the Seyfert 2's.

$b/a = 0.5 \pm 0.3$ ¹ contrasting with $b/a = 0.7 \pm 0.2$ for Seyfert 1 galaxies. These results are also supported by the observed correlation between continuum reddening and inclination of the host galaxy (Crenshaw & Kraemer 2001). Thus, host galaxy-related obscuration may contribute to the inclination dependence of the [O III] emission, although our sample is too small to draw strong conclusions.

Assuming a gas-to-dust ratio for the host galaxy of $5.2 \times 10^{21} \text{cm}^{-2} \text{mag}^{-1}$ (Shull & van Steenberg 1985) the additional absorbing column calculated from the values derived for extinction (A_v) is in the range of $N_H \sim (2 - 10) \times 10^{21} \text{cm}^{-2}$ for the Seyfert 2 galaxies. The median values for the X-ray hydrogen column densities for our Seyfert 2 and Seyfert 1 samples are $N_H = 2.1 \times 10^{23} \text{cm}^{-2}$ and $N_H = 1.2 \times 10^{21} \text{cm}^{-2}$, respectively (Tueller et al. 2007). The observed discrepancy between the X-ray column density and those required for the extinction of the [O III] emission lines is consistent with previous results (e.g., Maccacaro et al. 1982; Reichert et al. 1985; Maiolino et al. 2001). The X-ray column density is measured along the line of sight to the nucleus and the derived reddening measures the column density towards the NLR. Thus while different gas-to-dust ratios may contribute, it is also likely that there is an additional attenuating gas component closer to the X-ray source which is not affecting the [O III] emission, as first suggested by Maccacaro et al. (1982).

3.2. The Correlation Between [O III],[O IV] and the 2-10 keV Band

In Figure 2 we present comparisons between [O IV] and [O III] luminosities and X-ray (2-10 keV) and BAT (14-195 keV) luminosities. Linear fits to these relations, and statistical analysis are presented in Table 3. From the different relations, the lowest level of significance for a correlation is obtained for the [O IV] versus the 2-10 keV hard X-ray. We propose that comparing the heavily-absorbed hard X-ray band in Seyfert 2's with the “unabsorbed” [O IV] may have weakened any correlation. In order to corroborate this statement we used the relation, $L_{[\text{O IV}]} \propto L_{2-10\text{keV}}^{0.7 \pm 0.1}$, derived from the Seyfert 1's to estimate the hard X-ray 2-10 keV fluxes for the Seyfert 2 galaxies using their observed [O IV]. To investigate the effect of ionized absorption on the 2-10 keV X-ray continuum, we created a multiplicative table (mtable) model using the “grid” and “punch XSPEC” options (Porter et al. 2006) in the photoionization code CLOUDY, version 07.02.01, last described by Ferland et al. (1998). A single zone and simple power law incident continuum model was assumed, with photon index $\Gamma = 1.8$, and low- and high-energy cutoffs at 1 micron and 100 keV, respectively. Hydrogen

¹The values for the major and minor diameter of the host galaxy, a and b respectively, were taken from NED

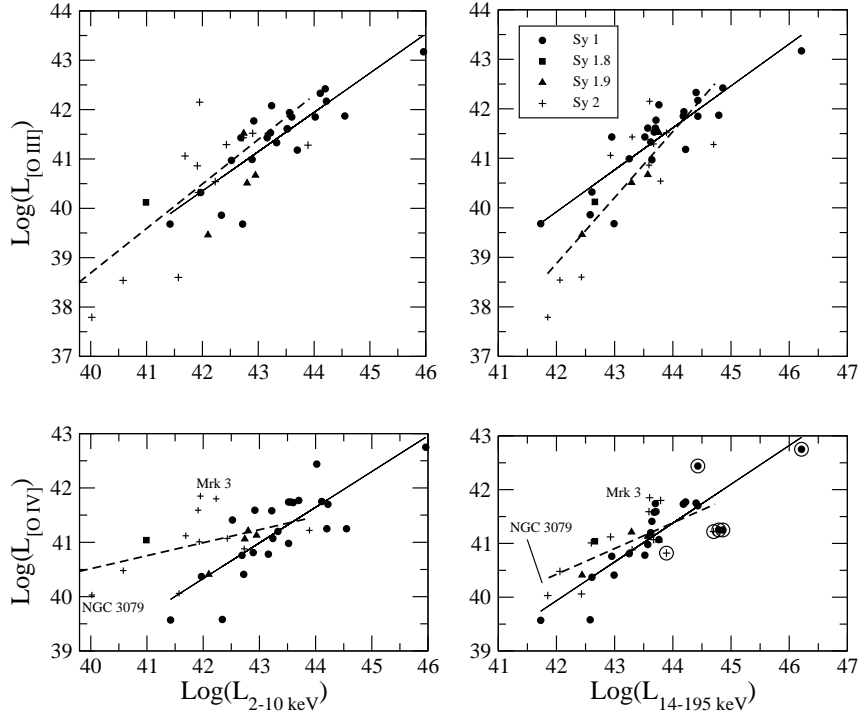


Fig. 2.— Correlation between [O IV] and [O III] luminosities with hard X-ray (2-10 keV) band and BAT (14-195 keV) luminosities. The solid line represents the linear regression calculated for the Seyfert 1 galaxies and the dashed line represents the linear regression for the Seyfert 2 galaxies. The circles in the lower right panel represent radio loud (RL) objects.

column density was then varied, with hydrogen number density fixed at $n_H = 10^8 \text{ cm}^{-3}$, and ionization parameter $\log(U) = -1$, where the ionization parameter U is defined as (see Osterbrock & Ferland 2006):

$$U = \frac{1}{4\pi R^2 c n_H} \int_{\nu_o}^{\infty} \frac{L_\nu}{h\nu} d\nu = \frac{Q(H)}{4\pi R^2 c n_H}, \quad (1)$$

where R is the distance to the cloud, c is the speed of light and $Q(H)$ is the flux of ionizing photons.

The resulting table was then fed into the X-ray spectral fitting package XSPEC (version 12.3.1). We reproduced the incident power law in XSPEC using the POWERLAW additive model, attenuated by absorption from the Cloudy-produced mtable. Using the XSPEC “flux” command, we determined the effect of various hydrogen column densities on the emergent 2-10 keV X-ray flux. Finally, we obtained the column densities needed in order to correct the observed hard X-ray fluxes with their intrinsic counterpart derived from the [O IV].

In Figure 3 we compare the predicted absorbing column densities with values found in the literature (Table 4). Even though we used a simple X-ray model, the predicted column densities are in good agreement with those from the literature. NGC 2992 is the evident outlier from our sample. The X-ray flux has been seen to vary dramatically throughout the history of NGC 2992 (Trippe et al., in preparation). As we mentioned before, the 2-10 keV fluxes are mainly from *ASCA* observations (in order to maintain consistency within our sample). *ASCA* observations for this object were taken in 1994 and *Spitzer* IRS staring observations in 2005. Using the hard X-ray flux, $f_{2-10\text{keV}} = 8.88 \times 10^{-11} \text{ ergs cm}^{-2} \text{ s}^{-1}$, observed by Murphy et al. (2007) with the *Rossi X-ray Timing Explorer* (RXTE) in 2005, we obtained better agreement with the absorbing column density predicted from the [O IV] (see Figure 3 and Table 4). Overall, these results confirm the heavy absorption present in Seyfert 2 galaxies and the effectiveness of [O IV] as a true indicator of the intrinsic X-ray luminosity of the galaxy.

The good empirical correlation between the [O III] emission line and the hard X-ray in the 2-10 keV band has been discussed extensively (e.g., Alonso-Herrero et al. 1997; Xu et al. 1999; Heckman et al. 2005; Netzer et al. 2006). This correlation is often used to determine the intrinsic X-ray luminosity, both in absorbed AGN where the observed X-ray flux is affected by absorption. We corroborate this in our sample, in that we find a strong linear correlation between [O III] and 2-10 keV luminosities. However, caution must be taken when using this correlation since [O III] and hard X-ray luminosities are essentially absorbed quantities, especially in Seyfert 2 sources. We suggest that the combined effect of extinction in the [O III] luminosities ($A_v \sim 1 - 6 \text{ mag}$) with correspondingly heavily absorbed 2-10 keV

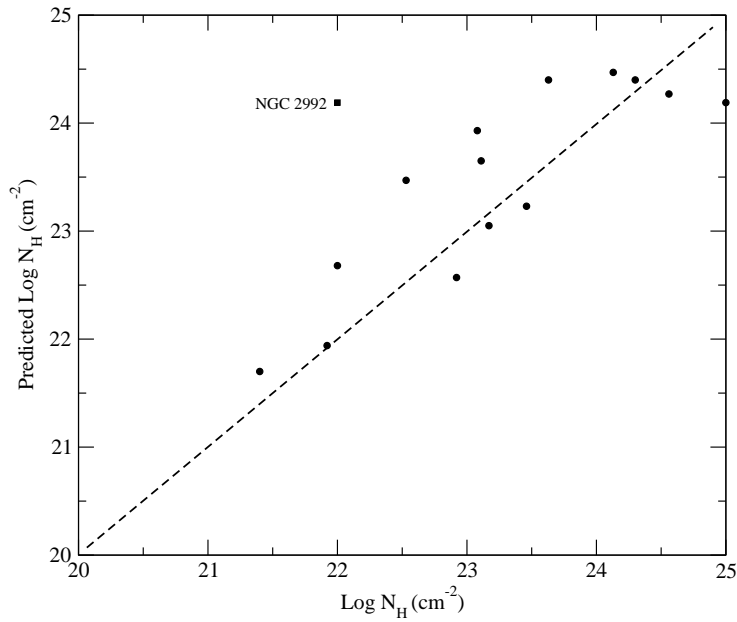


Fig. 3.— Comparison between the predicted absorbing column densities and values found in the literature for our Seyfert 2 population. The predicted values were derived using the [O IV] and 2-10 keV luminosity correlation found for Seyfert 1's. The square represents the column density prediction based on ASCA observations for the X-ray flux in 2004 for NGC 2992 (see text for details). The dashed line represents a 1:1 correspondence.

fluxes for Seyfert 2 galaxies results in a false correlation, thereby underestimating the true intrinsic luminosity of the AGN, particularly for nearly X-ray Compton thick sources.

3.3. The Correlation Between [O III], [O IV] and the BAT Band

Based on the statistical analysis we found equally good correlations for the [O III] and [O IV] relations with the 14-195 keV band. As we mentioned before, the [O IV] represents a relatively uncontaminated quantity and therefore the relation with an unabsorbed quantity such as the BAT fluxes should give the best correlation, assuming that the [O IV] is a good indicator of the power of the AGN. However, from the statistical analysis, this does not seem to be the case. To explore this behavior we applied linear regression fits to the individual Seyfert 1 and Seyfert 2 galaxies in our sample (see Figure 2).

The highest level of correlation was obtained for the Seyfert 1 galaxies: [O III] versus the 14-195 keV ($r_s = 0.88$, $P_r = 1.2 \times 10^{-7}$) and [O IV] versus the 14-195 keV ($r_s = 0.84$, $P_r = 3.6 \times 10^{-7}$). As we found previously, [O III] in Seyfert 2 galaxies is more affected by extinction than in Seyfert 1's. This could create a well-correlated linear distribution when comparing with the 14-195 keV BAT fluxes only if there is similar attenuation present in the 14-195 keV band for Seyfert 2's. Following the individual statistical analyses, Seyfert 2 objects have less correlated [O III] versus 14-195 keV hard X-ray ($r_s = 0.73$, $P_r = 1.6 \times 10^{-2}$) and [O IV] versus 14-195 keV hard X-ray luminosities ($r_s = 0.64$, $P_r = 3.4 \times 10^{-2}$) than Seyfert 1 galaxies. Partial absorption of the hard X-ray fluxes, especially in Seyfert 2 galaxies, with the relatively unobscured [O IV] is suggested as the cause for the low level of correlation. We found that, using $L_{[\text{O III}]} \propto L_{14-195\text{keV}}^{0.9 \pm 0.1}$ derived from the Seyfert 1 population, we underpredicted the BAT luminosities for the Seyfert 2 galaxies. This is an expected result considering the extinction of the [O III] emission. On the other hand, using the $L_{[\text{O IV}]} \propto L_{14-195\text{keV}}^{0.7 \pm 0.1}$ derived from the Seyfert 1 population, we overpredicted the BAT luminosities for most of the Seyfert 2 galaxies. There are two different scenarios to explain the over-prediction: an overestimation of [O IV] due to contamination from [Fe II] (see Section 2) and absorption in the 14-195 keV BAT band.

Although we cannot dismiss the former, we expect minimal starburst contribution in our X-ray selected sample. However, we are aware of the importance of [Fe II] emission especially in weak X-ray sources. In order to estimate the [Fe II] contamination coming from the starburst contribution we calculated the predicted [O IV] from the relation with the 14-195 keV luminosities for Seyfert 1 galaxies and compared with the observed [O IV] luminosities for two extreme Seyfert 2 objects (see Figure 2): NGC 3079, with a major contribution from the starburst (Gorjian et al. 2007), and Mrk 3, with no starburst (Deo et al. 2007).

Using these luminosities we estimated an upper limit for the [Fe II] starburst contribution to be ~ 1.5 times the uncontaminated [O IV] luminosity for the low-resolution spectra of NGC 3079. Comparing the full low-resolution with the full high-resolution IRS spectra obtained by Weedman et al. (2005) we clearly see [Fe II] as the dominant component (and the impossibility of resolving the [O IV] in the low-resolution spectra for NGC 3079). We also noticed that the strong [O IV] emission line in Mrk 3 shows no contribution from [Fe II]. However, the nearly X-ray Compton-thick Mrk 3 (Bianchi et al. 2005), with uncontaminated and unabsorbed [O IV], still overpredicts the measured BAT flux and the observed [O IV] of NGC 3079 is consistent with the X-ray flux, if the source is nearly X-ray Compton-thick (Cappi et al. 2006), as we showed with the XSPEC simulation.

Therefore, the most likely scenario to explain the hard X-ray overprediction in Seyfert 2's is partial absorption in the 14-195 keV BAT band. In order to investigate this last statement further we used, as before, the X-ray spectral fitting package XSPEC. For energies above 10 keV, we employed the standard XSPEC model PLCABS, which simulates attenuation of a power law continuum by dense, cold matter (Yaqoob 1997). The model grid has a high energy flux calculation limit of 50 keV, so our flux range was limited to 14-50 keV. To accommodate large column densities, we set the maximum number of scatterings considered by the model to a value of 12, as suggested by Yaqoob (1997). As before, the power law photon index was set to $\Gamma = 1.8$. Other variable model parameters were set to default values, and the column density was varied to determine relative changes in the predicted 14-50 keV X-ray luminosities using the [O IV]- BAT correlation for Seyfert 1's, and the observed BAT 14-50 keV X-ray luminosities of the Seyfert 2 galaxies. From these results, we derived a mean column density of $N_H \approx (3.2 \pm 0.8) \times 10^{24} \text{cm}^{-2}$ for our Seyfert 2 population. Given the energy limitation of the previous method, this result is in agreement with a derived value of $N_H \approx (2.4 \pm 0.8) \times 10^{24} \text{cm}^{-2}$, calculated using the average values for the predicted and the observed BAT X-ray luminosities, and assuming a purely Thomson cross-section. From this value of column density the BAT 14-195 keV X-ray band appear to have been partially absorbed. This result is in good agreement with the large column densities observed for Mrk 3 and NGC 3079 (see Table 4).

3.4. Radio Loudness and [O IV]

There is a well known linear correlation between the radio and the [O III] luminosities, and that this correlation is similar for both radio quiet and radio loud AGNs (e.g., Xu et al. 1999; Ho & Peng 2001). We noticed that some of the objects in our sample, which show more more scattered with respect to the linear correlation between [O IV] and BAT luminosities,

are radio loud sources (see Figure 2, open circles). In order to investigate whether or not this is an actual trend or a sample selection effect, we expanded our original sample to include more radio loud objects. We used the sample and radio loudness classification from Xu et al. (1999) and selected the objects that have been observed with *Spitzer* and are classified as Seyfert galaxies (following NED and SIMBAD classification). These new objects do not have 14-195 keV fluxes from the 9 month BAT survey and therefore are not included in any of the previous calculations regarding the correlations of the [O IV] and the hard X-ray. We obtained the [O IV] fluxes from the literature and *Spitzer* IRS staring mode archival (unpublished) spectra in low resolution. The extended sample is presented in Table 2 (the labels are the same as in Table 1).

The relationship between the [O III] and [O IV] has been studied before in powerful Fanaroff-Riley class II radio galaxies (Haas et al. 2005). Haas et al. (2005) found [O III] not to be a true indicator of the AGN, because the optical emission from the NLR suffers extinction. In Figure 4 we compare the [O IV] and [O III] luminosities for the combined sample, i.e. the original and extended sample. From the comparison it become clear that radio loud sources exhibit higher emission line luminosities than those of other types of active galaxies. This result is in agreement with previous findings and could be explained by a proposed bowshock model where part of the NLR emission is being powered by a radio-emitting jets, present in radio loud AGNs (eg. Taylor et al. 1992; Dopita & Sutherland 1995; Bicknell et al. 1997, 1998). Most of the radio loud objects included in the extended sample were chosen to be powerful radio sources (Haas et al. 2005; Ogle et al. 2006). Therefore, our results are hampered by selection effects. Furthermore, our small sample does not allow us to extract any statistically significant results to determine a clear trend that may distinguish between Type 1 and Type 2 radio loud AGNs. For example, there may be evidence for a high [O IV]/[O III] in radio loud Seyfert 1's, as suggested by Haas et al. (2005), however the same trend is not seen in the RL Seyfert 2 galaxies. This remains as an open question for further analysis.

4. Photoionization modeling

To investigate the physical conditions in the emission line regions for both the [O IV] and [O III], we generated single-zone, constant-density models. We used a set of roughly solar abundances (e.g., Grevesse & Anders 1989). The logs of the abundances relative to H by number are: He: -1; C: -3.46; N: -3.92; O: -3.19; Ne: -3.96; Na: -5.69; Mg: -4.48; Al: -5.53; Si: -4.50; P: -6.43; S: -4.82; Ar: -5.40; Ca: -5.64; Fe: -4.40 and Ni: -5.75. We assumed a column density of 10^{21}cm^{-2} , which is typical of the narrow line region (e.g., Kraemer et al.

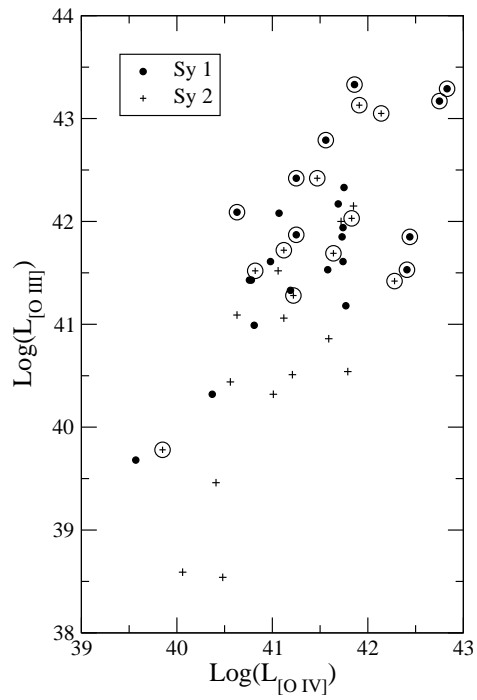


Fig. 4.— Correlation between [O IV] and [O III] luminosities for the combined sample, i.e. the original and extended sample. The circles represent radio loud (RL) objects. For the purpose of comparison we group Seyfert’s 1.8 and 1.9 with the Seyfert 2 galaxies.

2000). Although it is likely that there is dust mixed in with the emission-line gas in the NLRs of Seyfert galaxies (e.g., Kraemer & Harrington 1986; Netzer & Laor 1993), more recent studies using optical and UV long-slit spectra obtained with the Space Telescope Imaging Spectrograph aboard the *Hubble Space Telescope* indicate that the dust/gas ratios are significantly lower than in the Galactic ISM (Kraemer & Crenshaw 2000b,a; Kraemer et al. 2000). Therefore, we have not included dust in our models.

For the Spectral Energy Distribution (SED) we assume a broken power law as used by Kraemer et al. (2004) and similar to that suggested for NGC 5548 (Kraemer et al. 1998) and NGC 4151 (Kraemer et al. 2000) of the form $F_\nu \propto \nu^{-\alpha}$, with $\alpha=0.5$ below 13.6 eV, $\alpha=1.5$ from 13.6 eV to 1 keV and 0.8 at higher energies. We generated a grid of photoionization models varying the ionization parameter U and total hydrogen number density (n_H). The average BAT luminosity (14-195 keV) of the sample, 2.67×10^{43} ergs s⁻¹, yields a flux of ionizing photons of $Q(H) \sim 1.2 \times 10^{54}$ photons s⁻¹.

In order to study the physical conditions present in the emission-line regions, we need to use intrinsic quantities (free of viewing angle effects). As discussed in the previous section, the [O III] emission line seems to be more affected by reddening in Seyfert 2 than Seyfert 1 galaxies. Consequently, we used the values derived from the Seyfert 1 galaxies in our sample to constrain the photoionization parameters. We suggested that, given the isotropic properties for [O IV], the physical conditions derived from our Seyfert 1 population could be extended to Seyfert 2 as well.

From the Seyfert 1's we find that the average [O IV] and [O III] ratio is $\sim 1.0 \pm 0.2$. Assuming that the [O III] and [O IV] emission comes from the same gas, we used the generated grid of models to find the range in U and n_H for which we can obtain a ratio of approximately unity for different values of extinction (A_v). We obtained a range for the ionization parameter $-1.50 < \log(U) < -1.30$ and for the hydrogen density, $2.0 < \log(n_H) < 4.25$ (cm⁻³), assuming no extinction ($A_v = 0$). The values for n_H lie around the [O IV] critical density, $\log(n_c) \sim 3.7$, where the line intensity peaks. The critical density for the ²P₂^o level of O³⁺, which is the upper level of the [O IV] line, was calculated using the formalism described in Osterbrock & Ferland (2006) using atomic data from Blum & Pradhan (1992) and Galavis et al. (1998).

Baskin & Laor (2005) found from their single-zone approximation a relatively small range for the values of n_H ($\log(n_e) \sim 5.85 \pm 0.7$ cm⁻³)² and a relatively small range of U

² The photoionization code CLOUDY uses the total hydrogen density (n_H) instead of the electron density (n_e) as used by Baskin & Laor (2005). We assumed, in our simple model, both densities to be roughly the same.

($\log(U) = -3 \pm 0.5$) where both the [O III] and H β are emitted efficiently. For their two-zone model assuming $n_e = 10^3 \text{cm}^{-3}$ for the outer zone and $n_e = 10^7 \text{cm}^{-3}$ and $\log(U) = -1$ for the inner zone, they found higher U values for the outer zone than in the single-zone approximation ($-3.5 < \log(U) < -2$). These are typical values for the conditions in the NLR (e.g., Kraemer et al. 2000). While our models predicted higher ionization parameters than Baskin & Laor (2005), they did not attempt to include [O IV].

In Figure 5, we present the required parameter space to obtain a [O IV]/[O III] of unity for different values of A_v and compared with that found by Baskin & Laor (2005) in their single-zone model. This comparison shows the dependence of this ratio in terms of the ionization parameter, hydrogen density and extinction. For a higher extinction, the parameter space required is closer to that found by Baskin & Laor (2005), meaning that the intrinsic ratio is smaller than unity and therefore representing a region where the [O III] is dominant, relative to the [O IV] emission. In the absence of such large extinction ($A_v \gtrsim 6 \text{mag}$), it is likely that the [O IV] is coming from a more highly ionized and lower density gas. Our comparison of [O IV] and [O III] show that the single-zone model cannot reproduce the physical conditions present in the NLR gas since U would be too low to produce the observed [O IV] and the line would be collisionally suppressed. On the other hand, our results are in better agreement with the higher ionization state found in their constant density outer zone. However, this higher ionization and lower density cloud population cannot fully reproduce the observed [O IV].

Since U depends on the flux of ionizing photons ($Q(H)$), the distance to the source (R) and the hydrogen density of the gas (n_H), we used the model grid predictions to calculate a range for the distances to the source. Then, we determined a range for the covering factors (Cf) by adjusting to the observed [O IV] luminosity of the sample. We found a distance of the emitting gas from the central source of $250 \text{ pc} > R > 30 \text{ pc}$ and a range of covering factors of $0.04 < Cf < 0.15$. The range in parameter space in our grid was dominated by matter bounded models. In the matter bounded case, all the material is ionized and some fraction of the ionizing radiation passes through the gas unabsorbed. Therefore, the covering factor must be higher than that from a radiation bounded model (in which all the ionizing radiation is absorbed in the NLR), to account for the observed strength of the emission lines. However, the inclusion of dust in the models will decrease the size of the ionized zone, which would further increase the predicted covering factors (e.g., Netzer & Laor 1993; Baskin & Laor 2005). If the [O IV] arose in such dusty gas, it would imply higher covering factors than our models predict. Nevertheless, the results from our dust-free models are in good agreement with the Cf ($\sim 0.02 - 0.2$) obtained by Baskin & Laor (2005) in their radiation bounded dusty models. There is evidence for a component of high ionization matter bounded gas in the NLR in which optical lines such as [Ne V] $\lambda 3426$ and [Fe VII] $\lambda 6087$ form

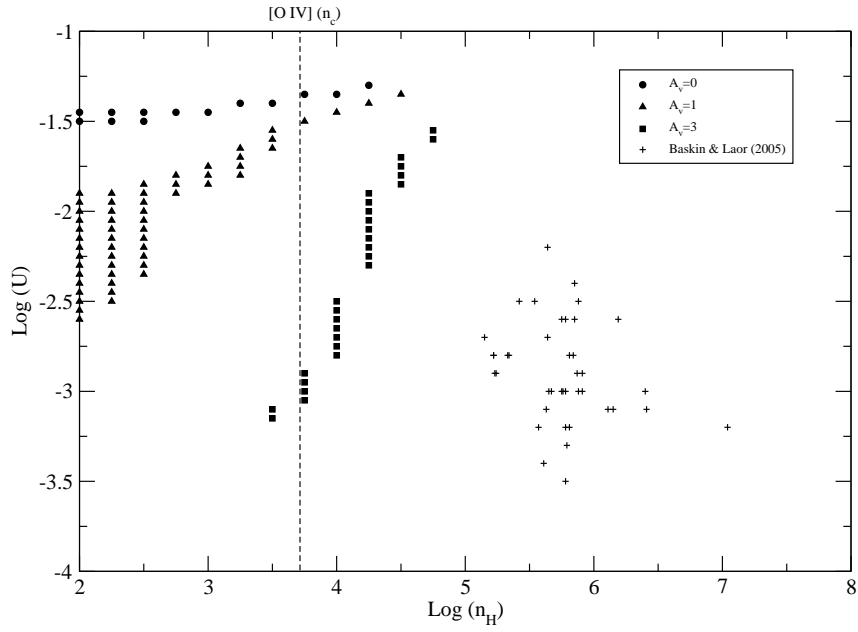


Fig. 5.— Comparison between the parameter space required to obtain a ratio of approximately unity for [O IV]/[O III] for different extinction magnitudes for the [O III]. For comparison we shown the parameter space obtained by Baskin & Laor (2005).

(e.g., Binette et al. 1996; Kraemer & Crenshaw 2000a; Kraemer et al. 2000), so it is likely that the [O IV] originates in the same gas, while most of the [O III] arises in conditions similar to those found by Baskin & Laor (2005).

In Figure 6 we present the photoionization model grid overlaid on the Seyfert 1 luminosities and the linear regression for all the sample. Each case corresponds to a different set of covering factors (Cf) for a distance from the ionizing source to the gas cloud of $R = 130$ pc. The model X-ray luminosities are calculated using U , the fixed radial distance, the range in densities shown in Figure 6, and our assumed SED (see Equation 1).

As presented in Figure 6, our simple photoionization model can reproduce the observed $L_{[\text{O IV}]}$ to $L_{14-195\text{keV}}$ relationship. In order to fit the higher luminosity sources, the models predict that more distant or higher density gas is required for the NLR. We dismiss the latter because, at high densities (i.e. higher than the critical density for [O IV]), the [O IV] is collisionally de-excited and the line intensity decreases. Therefore, the most likely scenario is a more distant NLR for high luminosity sources. On the other hand, Figure 6 shows that our simple photoionization model underpredicts [O IV] at $R = 130$ pc, even at low densities. Consequently, in the low luminosity sources the NLR must be fairly small ($R < 150$ pc) with a bigger covering factor ($Cf \gtrsim 0.07$), since gas at or below the critical density of the [O IV] would not be sufficiently ionized at large distances from the source. These results suggests that the size of the NLR scales with the luminosity of the source, in agreement with the observed good correlation between the NLR size and the luminosity of the AGN (Schmitt et al. 2003).

5. Conclusions

We have explored the relationship between the $L_{[\text{O IV}]}$ - $L_{14-195\text{keV}}$ and related correlations for a sample of X-ray selected nearby Seyfert Galaxies. For the X-ray selected sample the [O IV] and the [O III] luminosities are well-correlated with the hard X-ray luminosity in the 14-195 keV band over a range of ~ 3 and 5 orders of magnitude, respectively.

From the [O IV] and [O III] comparison we derived an absorbing column density from the reddening toward the NLR for Seyfert 2 galaxies, $N_H \sim (2 - 10) \times 10^{21}\text{cm}^{-2}$, which is smaller than the median value for the X-ray column densities, $N_H = 2.1 \times 10^{23}\text{cm}^{-2}$. The differences in the line of sight for the different absorbing columns are consistent with an additional attenuating gas component close to the X-ray source. We also suggested that part of the obscuration in the NLR of Seyfert 2 galaxies may occur in the disk of the host galaxy, given the fact that, in our sample, Seyfert 2 galaxies are on average more inclined.

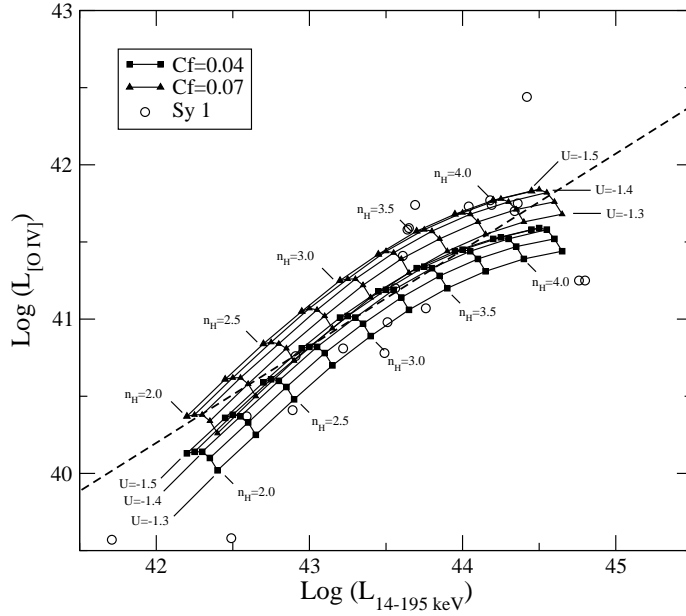


Fig. 6.— Comparison between the correlation of [O IV] luminosities with BAT X-ray luminosities and a grid of photoionization models for different covering factors (Cf) for a distance of $R = 130$ pc. The dashed line represents the linear regression obtained for the observed luminosities for all the sample and the open circles represent the observed Seyfert 1's luminosities (see Figure 2). n_H refers to the log of the hydrogen nucleus density and U to the log of the ionization parameter. The vertical dashed line indicates the critical density for the [O IV] line

We obtained a correlation between the $L_{[\text{O IV}]}-L_{2-10 \text{ keV}}$ that is not as strong as the one between $L_{[\text{O III}]}-L_{2-10 \text{ keV}}$, which results from comparing the heavily absorbed 2-10 keV band, especially in Seyfert 2 galaxies, with the intrinsic (unabsorbed) [O IV] fluxes. As pointed out in previous works, there is a good correlation between [O III] and hard X-ray 2-10 keV luminosities. However, we conclude that the combined effects of reddening in the [O III] and absorption in the 2-10 keV band may result in a false correlation.

For the $L_{[\text{O III}]}$ and $L_{[\text{O IV}]}$ relations with the $L_{14-195\text{keV}}$ BAT band we found equally good correlations. Using the linear regression found for Seyfert 1 galaxies we underpredict the hard X-ray 14-195 keV BAT luminosities of Seyfert 2's obtained from the $L_{[\text{O III}]}$ versus hard X-ray $L_{14-195\text{keV}}$ relation and overpredict the hard X-ray 14-195 keV BAT luminosities using the $L_{[\text{O IV}]}$ relation. We explain the former case due to the extinction of the [O III] ($A_v \sim 1 - 6 \text{ mag}$) and the latter with absorption in the BAT band. We found that for a column density of $N_H \sim 3 \times 10^{24} \text{ cm}^{-2}$ the BAT luminosities could be smaller, by a factor of $\sim 5 \pm 3$, than the intrinsic luminosities derived from the Seyfert 1's relation.

Assuming that the [O III] and [O IV] come from the same gas, and using the mean fluxes of the sample, we conclude that the emitting region for [O IV] is in a higher ionization state and lower density than the components modeled for the [O III] emitting region by Baskin & Laor (2005) and has a mean covering factor of $Cf \sim 0.07$. The physical conditions derived from the photoionization models indicate that [O IV] originates in the inner ~ 150 pc of the NLR.

In conclusion, we propose the [O IV] as a truly isotropic property of AGNs given its high ionization potential and that it is unaffected by reddening, which makes this line easy to identify and extract. This is true at least in galaxies with minimal or no star formation as for our X-ray selected sample. Where star formation activity has an important contribution this may not be the case, especially with contamination from [Fe II] $\lambda 25.99 \mu\text{m}$ in low-resolution IRS spectra. In a future work we will expand our sample to include the complete 22 month *SWIFT*/BAT survey and high resolution *Spitzer* IRS observations to continue to explore these open issues.

We would like to thank our anonymous referee for her/his insightful comments and suggestions that improved the paper. This research has made use of the NASA/IPAC Extragalactic Database (NED) which is operated by the Jet Propulsion Laboratory, California Institute of Technology, under contract with the National Aeronautics and Space Administration. The IRS was a collaborative venture between Cornell University and Ball Aerospace Corporation funded by NASA through the Jet Propulsion Laboratory and Ames Research Center. SMART was developed by the IRS Team at Cornell University and is available

through the Spitzer Science Center at Caltech. Basic research in astronomy at the NRL is supported by 6.1 base funding.

REFERENCES

- Adams, T. F., & Weedman, D. W. 1975, *ApJ*, 199, 19
- Akylas, A., Georgantopoulos, I., Griffiths, R. G., Papadakis, I. E., Mastichiadis, A., Warwick, R. S., Nandra, K., & Smith, D. A. 2002, *MNRAS*, 332, L23
- Alonso-Herrero, A., Ward, M. J., & Kotilainen, J. K. 1997, *MNRAS*, 288, 977
- Antonucci, R. 1993, *ARA&A*, 31, 473
- Antonucci, R. R. J., & Miller, J. S. 1985, *ApJ*, 297, 621
- Armus, L., Charmandaris, V., Bernard-Salas, J., Spoon, H. W. W., Marshall, J. A., Higdon, S. J. U., Desai, V., Teplitz, H. I., Hao, L., Devost, D., Brandl, B. R., Wu, Y., Sloan, G. C., Soifer, B. T., Houck, J. R., & Herter, T. L. 2007, *ApJ*, 656, 148
- Baskin, A., & Laor, A. 2005, *MNRAS*, 358, 1043
- Bassani, L., Dadina, M., Maiolino, R., Salvati, M., Risaliti, G., della Ceca, R., Matt, G., & Zamorani, G. 1999, *ApJS*, 121, 473
- Bianchi, S., Miniutti, G., Fabian, A. C., & Iwasawa, K. 2005, *MNRAS*, 360, 380
- Bicknell, G. V., Dopita, M. A., & O’Dea, C. P. O. 1997, *ApJ*, 485, 112
- Bicknell, G. V., Dopita, M. A., Tsvetanov, Z. I., & Sutherland, R. S. 1998, *ApJ*, 495, 680
- Binette, L., Wilson, A. S., & Storchi-Bergmann, T. 1996, *A&A*, 312, 365
- Blum, R. D., & Pradhan, A. K. 1992, *ApJS*, 80, 425
- Bonatto, C. J., & Pastoriza, M. G. 1997, *ApJ*, 486, 132
- Braatz, J. A., Wilson, A. S., & Henkel, C. 1997, *ApJS*, 110, 321
- Brotherton, M. S. 1996, *ApJS*, 102, 1
- Cappi, M., Panessa, F., Bassani, L., Dadina, M., Dicocco, G., Comastri, A., della Ceca, R., Filippenko, A. V., Gianotti, F., Ho, L. C., Malaguti, G., Mulchaey, J. S., Palumbo, G. G. C., Piconcelli, E., Sargent, W. L. W., Stephen, J., Trifoglio, M., & Weaver, K. A. 2006, *A&A*, 446, 459
- Cardelli, J. A., Clayton, G. C., & Mathis, J. S. 1989, *ApJ*, 345, 245

- Crenshaw, D. M., & Kraemer, S. B. 2001, *ApJ*, 562, L29
- Dadina, M. 2007, *A&A*, 461, 1209
- Dahari, O., & De Robertis, M. M. 1988, *ApJS*, 67, 249
- Deo, R. P., Crenshaw, D. M., Kraemer, S. B., Dietrich, M., Elitzur, M., Teplitz, H., & Turner, T. J. 2007, *ApJ*, 671, 124
- Dopita, M. A., & Sutherland, R. S. 1995, *ApJ*, 455, 468
- Elvis, M., Maccacaro, T., Wilson, A. S., Ward, M. J., Penston, M. V., Fosbury, R. A. E., & Perola, G. C. 1978, *MNRAS*, 183, 129
- Evans, D. A., Worrall, D. M., Hardcastle, M. J., Kraft, R. P., & Birkinshaw, M. 2006, *ApJ*, 642, 96
- Ferland, G. J., Korista, K. T., Verner, D. A., Ferguson, J. W., Kingdon, J. B., & Verner, E. M. 1998, *PASP*, 110, 761
- Galavis, M. E., Mendoza, C., & Zeippen, C. J. 1998, *A&AS*, 131, 499
- Gallo, L. C., Lehmann, I., Pietsch, W., Boller, T., Brinkmann, W., Friedrich, P., & Grupe, D. 2006, *MNRAS*, 365, 688
- Genzel, R., Lutz, D., Sturm, E., Egami, E., Kunze, D., Moorwood, A. F. M., Rigopoulou, D., Spoon, H. W. W., Sternberg, A., Tacconi-Garman, L. E., Tacconi, L., & Thatte, N. 1998, *ApJ*, 498, 579
- Gilli, R., Maiolino, R., Marconi, A., Risaliti, G., Dadina, M., Weaver, K. A., & Colbert, E. J. M. 2000, *A&A*, 355, 485
- Gorjian, V., Cleary, K., Werner, M. W., & Lawrence, C. R. 2007, *ApJ*, 655, L73
- Gregory, P. C., & Condon, J. J. 1991, *ApJS*, 75, 1011
- Grevesse, N., & Anders, E. 1989, in *American Institute of Physics Conference Series*, Vol. 183, *Cosmic Abundances of Matter*, ed. C. J. Waddington, 1–8
- Guainazzi, M., Matt, G., & Perola, G. C. 2005, *A&A*, 444, 119
- Haas, M., Siebenmorgen, R., Schulz, B., Krügel, E., & Chini, R. 2005, *A&A*, 442, L39
- Hartigan, P., Raymond, J., & Pierson, R. 2004, *ApJ*, 614, L69

- Heckman, T. M., Ptak, A., Hornschemeier, A., & Kauffmann, G. 2005, *ApJ*, 634, 161
- Higdon, S. J. U., Devost, D., Higdon, J. L., Brandl, B. R., Houck, J. R., Hall, P., Barry, D., Charmandaris, V., Smith, J. D. T., Sloan, G. C., & Green, J. 2004, *PASP*, 116, 975
- Ho, L. C., & Peng, C. Y. 2001, *ApJ*, 555, 650
- Horst, H., Smette, A., Gandhi, P., & Duschl, W. J. 2006, *A&A*, 457, L17
- Houck, J. R., Roellig, T. L., van Cleve, J., Forrest, W. J., Herter, T., Lawrence, C. R., Matthews, K., Reitsema, H. J., Soifer, B. T., Watson, D. M., Weedman, D., Huisjen, M., Troeltzsch, J., Barry, D. J., Bernard-Salas, J., Blacken, C. E., Brandl, B. R., Charmandaris, V., Devost, D., Gull, G. E., Hall, P., Henderson, C. P., Higdon, S. J. U., Pirger, B. E., Schoenwald, J., Sloan, G. C., Uchida, K. I., Appleton, P. N., Armus, L., Burgdorf, M. J., Fajardo-Acosta, S. B., Grillmair, C. J., Ingalls, J. G., Morris, P. W., & Teplitz, H. I. 2004, *ApJS*, 154, 18
- Isobe, N., Tashiro, M., Makishima, K., Iyomoto, N., Suzuki, M., Murakami, M. M., Mori, M., & Abe, K. 2002, *ApJ*, 580, L111
- Jackson, N., & Browne, I. W. A. 1991, *MNRAS*, 250, 422
- Keel, W. C. 1980, *AJ*, 85, 198
- Keel, W. C., de Grijp, M. H. K., Miley, G. K., & Zheng, W. 1994, *A&A*, 283, 791
- Khachikian, E. Y., & Weedman, D. W. 1974, *ApJ*, 192, 581
- Kraemer, S. B., & Crenshaw, D. M. 2000a, *ApJ*, 532, 256
- . 2000b, *ApJ*, 544, 763
- Kraemer, S. B., Crenshaw, D. M., Filippenko, A. V., & Peterson, B. M. 1998, *ApJ*, 499, 719
- Kraemer, S. B., Crenshaw, D. M., Hutchings, J. B., Gull, T. R., Kaiser, M. E., Nelson, C. H., & Weistrop, D. 2000, *ApJ*, 531, 278
- Kraemer, S. B., George, I. M., Crenshaw, D. M., & Gabel, J. R. 2004, *ApJ*, 607, 794
- Kraemer, S. B., & Harrington, J. P. 1986, *ApJ*, 307, 478
- Lutz, D., Maiolino, R., Spoon, H. W. W., & Moorwood, A. F. M. 2004, *A&A*, 418, 465
- Maccacaro, T., Perola, G. C., & Elvis, M. 1982, *ApJ*, 257, 47

- Maiolino, R., Marconi, A., Salvati, M., Risaliti, G., Severgnini, P., Oliva, E., La Franca, F., & Vanzi, L. 2001, *A&A*, 365, 28
- Maiolino, R., & Rieke, G. H. 1995, *ApJ*, 454, 95
- Markwardt, C. B., Tueller, J., Skinner, G. K., Gehrels, N., Barthelmy, S. D., & Mushotzky, R. F. 2005, *ApJ*, 633, L77
- Matt, G., Guainazzi, M., Maiolino, R., Molendi, S., Perola, G. C., Antonelli, L. A., Bassani, L., Brandt, W. N., Fabian, A. C., Fiore, F., Iwasawa, K., Malaguti, G., Marconi, A., & Poutanen, J. 1999, *A&A*, 341, L39
- Mulchaey, J. S., Koratkar, A., Ward, M. J., Wilson, A. S., Whittle, M., Antonucci, R. R. J., Kinney, A. L., & Hurt, T. 1994, *ApJ*, 436, 586
- Murphy, K. D., Yaqoob, T., & Terashima, Y. 2007, *ApJ*, 666, 96
- Netzer, H., & Laor, A. 1993, *ApJ*, 404, L51
- Netzer, H., Mainieri, V., Rosati, P., & Trakhtenbrot, B. 2006, *A&A*, 453, 525
- Ogle, P., Whysong, D., & Antonucci, R. 2006, *ApJ*, 647, 161
- O’Halloran, B., Satyapal, S., & Dudik, R. P. 2006, *ApJ*, 641, 795
- Osterbrock, D. E., & Ferland, G. J. 2006, *Astrophysics of gaseous nebulae and active galactic nuclei* (Astrophysics of gaseous nebulae and active galactic nuclei, 2nd. ed. by D.E. Osterbrock and G.J. Ferland. Sausalito, CA: University Science Books, 2006)
- Polletta, M., Bassani, L., Malaguti, G., Palumbo, G. G. C., & Caroli, E. 1996, *ApJS*, 106, 399
- Porter, R. L., Ferland, G. J., Kraemer, S. B., Armentrout, B. K., Arnaud, K. A., & Turner, T. J. 2006, *PASP*, 118, 920
- Rawlings, S., Saunders, R., Eales, S. A., & Mackay, C. D. 1989, *MNRAS*, 240, 701
- Reichert, G. A., Mushotzky, R. F., Holt, S. S., & Petre, R. 1985, *ApJ*, 296, 69
- Rhee, J. H., & Larkin, J. E. 2005, *ApJ*, 620, 151
- Risaliti, G., Maiolino, R., & Salvati, M. 1999, *ApJ*, 522, 157
- Schmitt, H. R., Antonucci, R. R. J., Ulvestad, J. S., Kinney, A. L., Clarke, C. J., & Pringle, J. E. 2001, *ApJ*, 555, 663

- Schmitt, H. R., Donley, J. L., Antonucci, R. R. J., Hutchings, J. B., Kinney, A. L., & Pringle, J. E. 2003, *ApJ*, 597, 768
- Shull, J. M., & van Steenberg, M. E. 1985, *ApJ*, 294, 599
- Steiner, J. E. 1981, *ApJ*, 250, 469
- Sturm, E., Lutz, D., Verma, A., Netzer, H., Sternberg, A., Moorwood, A. F. M., Oliva, E., & Genzel, R. 2002, *A&A*, 393, 821
- Tadhunter, C. N., Morganti, R., di Serego-Alighieri, S., Fosbury, R. A. E., & Danziger, I. J. 1993, *MNRAS*, 263, 999
- Taylor, D., Dyson, J. E., & Axon, D. J. 1992, *MNRAS*, 255, 351
- Tueller, J., Mushotzky, R. F., Barthelmy, S., Cannizzo, J. K., Gehrels, N., Markwardt, C. B., Skinner, G. K., & Winter, L. M. 2007, *ArXiv e-prints*, 711
- Turner, T. J., George, I. M., Nandra, K., & Mushotzky, R. F. 1997, *ApJ*, 488, 164
- Turner, T. J., Nandra, K., Turcan, D., & George, I. M. 2001, *X-ray Astronomy: Stellar Endpoints, AGN, and the Diffuse X-ray Background*, 599, 991
- Vignati, P., Molendi, S., Matt, G., Guainazzi, M., Antonelli, L. A., Bassani, L., Brandt, W. N., Fabian, A. C., Iwasawa, K., Maiolino, R., Malaguti, G., Marconi, A., & Perola, G. C. 1999, *A&A*, 349, L57
- Ward, M., Penston, M. V., Blades, J. C., & Turtle, A. J. 1980, *MNRAS*, 193, 563
- Weedman, D. W., Hao, L., Higdon, S. J. U., Devost, D., Wu, Y., Charmandaris, V., Brandl, B., Bass, E., & Houck, J. R. 2005, *ApJ*, 633, 706
- Whittle, M. 1992, *ApJS*, 79, 49
- Winkler, H. 1992, *MNRAS*, 257, 677
- Xu, C., Livio, M., & Baum, S. 1999, *AJ*, 118, 1169
- Yaqoob, T. 1997, *ApJ*, 479, 184
- Yee, H. K. C. 1980, *ApJ*, 241, 894

Table 1. Sample of Seyfert Galaxies

| Name | Type | z | $\log(L_{[\text{O III}]})$ | Luminosities (ergs s ⁻¹) | | | Remarks |
|-------------|------|----------|----------------------------|--------------------------------------|----------------------------|------------------------------|---------|
| | | | | $\log(L_{[\text{O IV}]})$ | $\log(L_{2-10\text{keV}})$ | $\log(L_{14-195\text{keV}})$ | |
| 3C120 | 1 | 0.033010 | 41.85 ^a | 42.44 | 44.02 | 44.43 | L |
| 3C273 | 1 | 0.158339 | 43.17 ^a | 42.75 | 45.96 | 46.21 | L |
| 3C382 | 1 | 0.057870 | 41.87 ^b | 41.25 | 44.55 | 44.79 | L |
| 3C390.3 | 1 | 0.056100 | 42.42 ^b | 41.25 | 44.20 | 44.86 | L |
| 3C452 | 2 | 0.081100 | 41.28 ^b | 41.22 | 43.89 | 44.70 | L |
| 3C84 | 2 | 0.017559 | 41.52 ^c | 40.82 | 42.90 | 43.89 | L |
| Circinus | 2 | 0.001448 | 38.54 ^c | 40.48 ^l | 40.58 | 42.06 | Q |
| ESO103-G035 | 1.9 | 0.013286 | 40.67 ^d | 41.13 | 42.95 | 43.57 | ... |
| IC4329a | 1.2 | 0.016054 | 41.18 ^d | 41.77 | 43.70 | 44.22 | Q |
| Mrk 6 | 1.5 | 0.018813 | 41.77 ^e | 41.59 ^k | 42.92 | 43.71 | ... |
| Mrk 79 | 1.2 | 0.022189 | 41.61 ^e | 41.74 ^k | 43.52 | 43.7 | Q |
| Mrk 348 | 2 | 0.015034 | 41.29 ^e | 41.07 ^k | 42.43 | 43.67 | ... |
| Mrk 3 | 2 | 0.013509 | 42.15 ^e | 41.85 | 41.95 | 43.6 | Q |
| Mrk 509 | 1.2 | 0.034397 | 42.33 ^f | 41.75 | 44.11 | 44.40 | Q |
| MCG-6-30-15 | 1.5 | 0.007749 | 39.68 ^m | 40.41 ^k | 42.72 | 42.99 | ... |
| MCG-2-58-22 | 1.5 | 0.046860 | 42.17 ^h | 41.70 | 44.22 | 44.43 | Q |
| NGC 1365 | 1.8 | 0.005457 | 40.12 ^d | 41.04 | 40.99 | 42.66 | ... |
| NGC 2992 | 2 | 0.007710 | 41.06 ⁱ | 41.12 | 41.69 | 42.93 | Q |
| NGC 3079 | 2 | 0.003723 | 37.79 ^j | 40.03 ^k | 40.02 | 41.85 | I |
| NGC 3227 | 1.5 | 0.003859 | 40.32 ^e | 40.37 ^k | 41.97 | 42.61 | Q |
| NGC 3516 | 1.5 | 0.008836 | 40.99 ^e | 40.81 ^k | 42.89 | 43.25 | Q |
| NGC 3783 | 1.5 | 0.009730 | 41.43 ^g | 40.78 | 43.16 | 43.52 | Q |
| NGC 4051 | 1.5 | 0.002336 | 39.68 ^g | 39.57 ^k | 41.42 | 41.73 | Q |
| NGC 4151 | 1.5 | 0.003319 | 41.43 ^g | 40.76 ^k | 42.69 | 42.95 | Q |
| NGC 4388 | 2 | 0.008419 | 40.86 ^g | 41.59 | 41.91 | 43.59 | Q |
| NGC 4507 | 1.9 | 0.011801 | 41.52 ^g | 41.06 | 42.74 | 43.76 | Q |
| NGC 526A | 1.5 | 0.019097 | 41.33 ^g | 41.20 ^k | 43.33 | 43.62 | Q |
| NGC 5506 | 1.9 | 0.006181 | 40.51 ^g | 41.21 | 42.80 | 43.29 | Q |
| NGC 5548 | 1.5 | 0.017175 | 41.61 ^e | 40.98 ^k | 43.52 | 43.57 | Q |
| NGC 6240 | 2 | 0.024480 | 40.54 ^c | 41.80 | 42.23 | 43.79 | Q |
| NGC 6300 | 2 | 0.003699 | 38.60 ^c | 40.06 | 41.57 | 42.43 | Q |
| NGC 7172 | 2 | 0.008683 | 41.43 ^d | 40.88 ^k | 42.73 | 43.30 | ... |
| NGC 7213 | 1.5 | 0.005839 | 39.86 ^d | 39.58 | 42.34 | 42.58 | ... |
| NGC 7314 | 1.9 | 0.004763 | 39.46 ^g | 40.41 ^k | 42.10 | 42.44 | Q |

Table 1—Continued

| Name | Type | z | Luminosities (ergs s ⁻¹) | | | | Remarks |
|------------|------|----------|--------------------------------------|---------------------------|----------------------------|------------------------------|---------|
| | | | $\log(L_{[\text{O III}]})$ | $\log(L_{[\text{O IV}]})$ | $\log(L_{2-10\text{keV}})$ | $\log(L_{14-195\text{keV}})$ | |
| NGC 7469 | 1.5 | 0.016317 | 41.53 ^g | 41.58 | 43.22 | 43.68 | Q |
| NGC 7582 | 2 | 0.005254 | 40.32 ^g | 41.01 | 41.93 | 42.60 | Q |
| NGC 931 | 1.5 | 0.016652 | 40.97 ^d | 41.41 ^k | 42.52 | 43.64 | ... |
| NGC 985 | 1 | 0.043143 | 41.94 ^g | 41.74 | 43.56 | 44.19 | Q |
| PG1501+106 | 1.5 | 0.036420 | 41.85 ^h | 41.73 | 43.60 | 44.18 | Q |
| PG1534+580 | 1 | 0.029577 | 42.08 ^g | 41.07 | 43.24 | 43.76 | Q |

Note. — The luminosities were calculated from the fluxes using $H_o = 71\text{kms}^{-1}\text{Mpc}^{-1}$ and a deceleration parameter $q_o = 0$ with redshift values taken from NED. The [O IV] luminosities obtained in the present work are presented in the table without references. The 2-10 keV fluxes are from ASCA observations and were retrieve from the TARTARUS data base (Turner et al. 2001) except for: 3C 84 from *XMM-Newton* observations (Evans et al. 2006); 3C 452 from *Chandra* ACIS observations (Isobe et al. 2002); MCG -2-58-22 and NGC 6300 from *BeppoSAX* MECS observations (Dadina 2007); Mrk 79 from *XMM-Newton* (Gallo et al. 2006); Mrk 79, which is from an *Ariel 5* observations (Elvis et al. 1978); NGC 3079 which is from *XMM-Newton* (Cappi et al. 2006). The 14-195 keV fluxes presented in this table are from the 9 months *SWIFT*/BAT high Galactic latitude survey (Tueller et al. 2007) except for: Circinus and NGC 3079, which are from Tueller et al. (in preparation). The last column follow the radio loudness classification from Xu et al. (1999), L= Radio loud, Q= Radio quiet and I= Intermediate.

References. — (a) Tadhunter et al. (1993), (b) Rawlings et al. (1989), (c) Polletta et al. (1996) , (d) Bonatto & Pastoriza (1997) and references therein , (e) Adams & Weedman (1975), (f) Yee (1980), (g) Whittle (1992) and references therein,(h) Dahari & De Robertis (1988), (i) Ward et al. (1980), (j) Braatz et al. (1997),(k) Deo et al. (2007),(l) Sturm et al. (2002), (m)Winkler (1992).

Table 2. Extended Sample

| Name | Type | z | Luminosities (ergs s ⁻¹) | | | Remarks |
|--------------|------|----------|--------------------------------------|---------------------------|----------------------------|---------|
| | | | $\log(L_{[\text{O III}]})$ | $\log(L_{[\text{O IV}]})$ | $\log(L_{2-10\text{keV}})$ | |
| 3C 109 | 1.8 | 0.305600 | 43.13 ^a | 41.91 ^j | 45.19 | L |
| 3C 192 | 2 | 0.059709 | 41.72 ^a | 41.12 | ... | L |
| 3C 234 | 1 | 0.184800 | 43.29 ^a | 42.83 ^k | 44.19 | L |
| 3C 249.1 | 1 | 0.311500 | 43.33 ^b | 41.86 ^j | 44.79 | L |
| 3C 321 | 2 | 0.096100 | 41.69 ^c | 41.64 ^j | 42.78 | L |
| 3C 323.1 | 1 | 0.264300 | 42.80 ^d | 41.56 ^j | 45.01 | L |
| 3C 33 | 2 | 0.059700 | 42.03 ^a | 41.83 ^k | 43.79 | L |
| 3C 381 | 1 | 0.160500 | 41.53 ^a | 42.41 ^k | ... | L |
| 3C 433 | 2 | 0.101600 | 41.42 ^e | 42.28 ^k | 44.08 | L |
| 3C 445 | 1 | 0.056200 | 42.09 ^f | 40.63 ^j | 43.76 | L |
| 3C 459 | 2 | 0.219900 | 42.42 ^f | 41.47 ^j | ... | L |
| 3C 79 | 2 | 0.255900 | 43.05 ^a | 42.14 ^j | ... | L |
| Mrk 231 | 1 | 0.042170 | 41.94 ^g | 41.42 ^l | 43.76 | I |
| Mrk 573 | 2 | 0.017179 | 42.00 ^h | 41.72 ^m | 41.25 | Q |
| NGC 5643 | 2 | 0.003999 | 40.44 ^h | 40.56 ^m | 40.35 | Q |
| NGC 6251 | 2 | 0.024710 | 39.78 ⁱ | 39.85 | 42.28 | L |
| TOL 0109-383 | 2 | 0.011764 | 41.09 ⁱ | 40.63 ^m | 41.72 | Q |

Note. — The luminosities were calculated from the fluxes using $H_0 = 71\text{kms}^{-1}\text{Mpc}^{-1}$ and a deceleration parameter $q_0 = 0$ with redshift values taken from NED. The [O IV] luminosities obtained in the present work are presented in the table without references. The 2-10 keV fluxes are from ASCA observations and were retrieved from the TARTARUS data base (Turner et al. 2001) except for: 3C 33 from *XMM-Newton* observations (Evans et al. (2006)); Mrk 573 from *XMM-Newton* observations (Guainazzi et al. 2005) and TOL 0109-383 from Heckman et al. (2005). The last column follows the radio loudness classification from Xu et al. (1999), L= Radio loud, Q= Radio quiet and I= Intermediate.

References. — (a) Rawlings et al. (1989), (b) Jackson & Browne (1991), (c) Gregory & Condon (1991), (d) Brotherton (1996), (e) Steiner (1981), (f) Tadhunter et al. (1993), (g) Dahari & De Robertis (1988), (h) Whittle (1992), (i) Polletta et al. (1996), (j) Haas et al. (2005), (k) Ogle et al. (2006), (l) Armus et al. (2007), (m) Sturm et al. (2002).

Table 3. Linear regressions and statistical analysis for the [O IV] and [O III] to their X-ray luminosities

| | $\log(L_{2-10\text{keV}})$ | | $\log(L_{14-195\text{keV}})$ | |
|---------------------------|---|------------|---|------------|
| | a | b | a | b |
| $\log L_{[\text{O III}]}$ | 0.82626 | 5.6382 | 1.0771 | -5.8703 |
| | 0.8 ± 0.1 | 5 ± 4 | 1.1 ± 0.1 | -6 ± 5 |
| | $r_s = 0.791, P_r = 7.8 \times 10^{-7}$ | | $r_s = 0.825, P_r = 2.5 \times 10^{-7}$ | |
| $\log L_{[\text{O IV}]}$ | 0.38903 | 24.467 | 0.61487 | 14.358 |
| | 0.4 ± 0.1 | 24 ± 3 | 0.6 ± 0.1 | 14 ± 3 |
| | $r_s = 0.596, P_r = 2.0 \times 10^{-4}$ | | $r_s = 0.798, P_r = 6.3 \times 10^{-7}$ | |

Note. — a and b represent the regression coefficient (slope) and regression constant (intercept) respectively. r_s is the Spearman rank order correlation coefficient and P_r is the null probability. For each relation we presented the exact linear regression values, the values as constrained by their statistical errors and the Spearman rank and null probability.

Table 4. Column densities for Seyfert 2 galaxies.

| Name | $\log N_H$ (XSPEC) | $\log N_H$ |
|-------------|--------------------|--------------------|
| Circinus | 24.27 | 24.56 ^a |
| ESO103-G035 | 23.05 | 23.17 ^b |
| Mrk 348 | 23.65 | 23.11 ^c |
| Mrk 3 | 24.47 | 24.13 ^d |
| NGC 2992 | 22.68 | 22.00 ^e |
| NGC 3079 | 24.19 | 25.00 ^f |
| NGC 4388 | 24.40 | 23.63 ^g |
| NGC 4507 | 23.23 | 23.46 ^g |
| NGC 5506 | 23.47 | 22.53 ^g |
| NGC 6240 | 24.40 | 24.30 ^h |
| NGC 6300 | 21.70 | 21.40 ⁱ |
| NGC 7172 | 22.57 | 22.92 ^b |
| NGC 7314 | 21.94 | 21.92 ^b |
| NGC 7582 | 23.93 | 23.08 ^g |

Note. — The XSPEC calculations are based on the comparison between [O IV] predictions and observed hard X-ray 2-10 keV fluxes. See text for details.

References. — (a) Matt et al. (1999), (b) ASCA observations retrieved using TARTARUS data base, (c) Akylas et al. (2002), (d) Bianchi et al. (2005), (e) Gilli et al. (2000), (f) Cappi et al. (2006), (g) Bassani et al. (1999), (h) Vignati et al. (1999), (i) Dadina (2007)